In vitro and in vivo behavior of ketoprofen intercalated into layered double hydroxides

Mihaela Silion · Doina Hritcu · Irina M. Jaba · Bogdan Tamba · Dunarea Ionescu · Ostin C. Mungiu · Ionel Marcel Popa

Abstract Ketoprofen (Ket) was intercalated into layered double hydroxides (ZnAlLDH and MgAlLDH) using the ionic exchange method. The drug intercalation was confirmed by X-ray diffraction (XRD) and FTIR spectroscopy. Ket release from the inorganic matrix was studied at pH 7.4 in continuous regime with a flow rate of 0.5 and respectively 1.0 ml/min. The kinetical data were interpreted using the Ritger and Peppas model. The data prove that the release kinetics and mechanism depend on the eluent flow rate. Quantification of gastric tolerance shows that the ulcerogenic effect of the intercalated drug is lower than the one of the raw Ket. The antinociceptive effect of both formulations was studied by the hot-plate method performed on mice. The MgAlLDH_Ket formulation shows a tendency towards a stronger antinociceptive effect than its ZnAlLDH_Ket counterpart during the 210 min recorded period.

1 Introduction

Ketoprofen (Ket), 2-(3-benzoylphenyl)-propionic acid, is an analgesic, antipyretic and a non-steroidal anti-inflammatory drug (NSAID) used for the treatment of rheumatoid arthritis, osteoarthritis and other chronic musculoskeletal conditions [1–3]. Conventional dosage forms of this drug, administered orally, three or four doses per day, have side effects such as peptic ulceration or bleeding and anorexia, and some additional side effects [4–6] that limit the use of Ket. These disadvantages added to the very short half-life, render Ket as a very good candidate for the production of controlled release formulations. Controlled release of the drug is expected to significantly mitigate these harmful systemic effects. Synthetic and natural polymeric or inorganic supports are currently used for designing controlled release drug systems [7–12]. Among these, the layered double hydroxides (LDHs) are attractive materials for the preparation of controlled release formulations. The general formula of LDHs can be expressed as $[M^{II}_{(1-x)}M^{III}_x(OH)_2]^{x+}A^{z-}_{x/z} \cdot nH_2O$, where M^{II} and M^{III} are divalent and trivalent cations, and A^{z-} is a group such as NO_3^-, Cl^-, OH^-, CO_3^{2-}, etc. that can be exchanged with organic anions. The x value, i.e., the charge density, is equal to the molar ratio $M^{3+}/(M^{2+} + M^{3+})$.

The large variety of anions that can be incorporated in the layered double hydroxides and their high anionic exchange capacity of these materials allow their use as matrices for tailoring specific organic–inorganic hybrid nanostructures with new potential applications such as: designing new pharmaceutics and new biocompatible materials. They are used as inorganic supports in the preparation of new pharmaceutical compositions by intercalation of non-steroidal anti-inflammatory drugs such as ibuprofen, diclofenac, indometacin, fenbufen, salicylic acid [13–19].

Previous in vivo pharmacological studies on rodents show that pharmaceuticals prepared by drug intercalation in the LDH show a synergic effect. On one hand the

M. Silion
Petru Poni Institute of Macromolecular Chemistry Iasi,
Aleea Grigore Ghica Voda 41A, 700487 Iasi, Romania

D. Hritcu · I. M. Popa (✉)
Faculty of Chemical Engineering and Environmental Protection,
Technical University Gh. Asachi, D. Mangeron Boulevard,
700050 Iasi, Romania
e-mail: mipopa@ch.tuiasi.ro

I. M. Jaba · B. Tamba · D. Ionescu · O. C. Mungiu
Center for the Study and Therapy of Pain, Gr. T. Popa University
of Medicine and Pharmacy Iasi, Strada Universitatii 16,
700115 Iasi, Romania

presence of the layered double hydroxides ensures a buffered environment and on the other hand it reduces the ulcerating side effects of the intercalated drug [14, 20, 21]. Besides these properties, LDHs were used because of their capability to prevent taurocholate induced gastric injury in rat that was earlier demonstrated and reported in the literature and this is another reason for choosing them as hosts in the present study [22].

In this paper we report in vitro and in vivo behavior of Ket intercalated into LDHs by ion-exchange method [23] using two matrices (MgAlLDH and ZnAlLDH) under various experimental conditions [24].

2 Materials and methods

2.1 Materials

All chemicals including $Zn(NO_3)_2 \times 6H_2O$, $Al(NO_3)_3 \times 9H_2O$, $Mg(NO_3)_2 \times 6H_2O$, and Ket were reagent grade (>98% purity), purchased from Sigma-Aldrich and were used without further purification. De-ionised water was used for the preparation of aqueous solutions.

2.2 Synthesis of precursor hydrotalcites

The precursor ZnAlLDH and MgAlLDH were prepared by a pH controlled co-precipitation technique of the corresponding metal nitrate salts at room temperature. In the case of ZnAlLDH, a solution containing 0.2 mol of $Zn(NO_3)_2 \times 6H_2O$ and 0.1 mol of $Al(NO_3)_3 \times 9H_2O$ in 300 ml of distilled water was added drop wise together with 1 M NaOH solution, under vigorous stirring. For MgAlLDH preparation, an aqueous solution containing 0.24 mol of $Mg(NO_3)_2 \times 6H_2O$ and 0.12 mol of $Al(NO_3)_3 \times 9H_2O$ was added drop wise together with 1 M NaOH aqueous solution, under vigorous stirring.

In both processes the solution flow rates are automatically adjusted in order to maintain a constant pH of 8.5 for ZnAlLDH and respectively 9.5 for MgAlLDH using a TitraLab TIM 854 apparatus. The suspensions were heated for 12 h at 65°C with vigorous stirring, then the solid precipitate was collected by filtration and washed 3–5 times with 25 ml aliquots of deionized water. The removal of leftover salt in the washing step was verified by conductometric analysis of the supernatant. The material was then dried at 65°C in vacuum.

2.3 Preparation of Ket intercalated hydrotalcites

ZnAlLDH_Ket and MgAlLDH_Ket were prepared using the anionic exchange method. Typically, 1 g ZnAlLDH or

MgAlLDH was dispersed in 150 ml H_2O and placed in a three-neck round bottom flask and degassed with nitrogen for 20 min. 1 M NaOH solution was then added until pH reached 8.5 for ZnAlLDH and respectively 9.5 for MgAlLDH. 150 ml hydro-alcoholic solution (50/50 v/v) containing 1.25 g dissolved Ket was then added to the previous mixture and stirred vigorously at 60°C for 16 h under nitrogen blanket in order to avoid atmospheric carbonate contamination. The solids were washed 3 to 5 times with 25 ml aliquots of distilled water. The completeness of the washing step was verified by the absence of free Ket in the spectrophotometric analysis. The resulting solids were vacuum-dried and used for subsequent investigation.

2.4 Determination of intercalated Ket content

Two methods were used for estimating Ket content of the composite samples: elemental analysis and spectrophotometric technique. For elemental analysis two methods were used: Pregl and Kjeldhal. In the spectrophotometric analysis a known amount of LDHs_Ket was dissolved 6 M HCl and diluted successively with phosphate buffer pH 7.2. The absorbance was measured at $\lambda = 255$ nm (this is the wavelength of maximum absorption for Ket, verified both in distilled water and in the respective buffer solution); the amount of intercalated Ket was calculated using a calibration curve (Fig. 1). For the calibration curve the data were generated using nine aqueous Ket solutions with concentrations in the range of 10 to 90 μg/ml, preparted by diluting a stock solution of Ket (1 mg/ml).

Three measurements were averaged for each data point and the equation of the calibration curve obtained by the least-square method was:

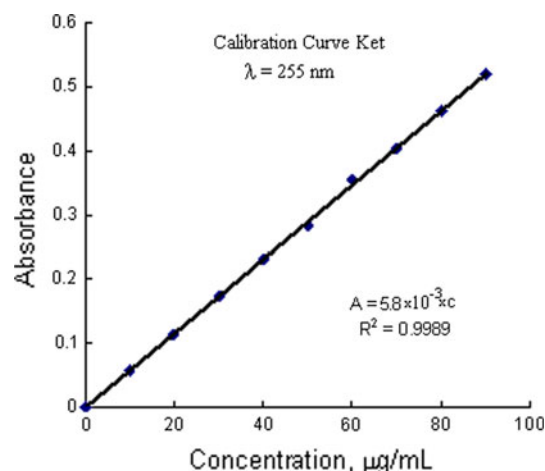$$A = 5.8 \times 10^{-3} \times c \qquad (1)$$

Fig. 1 Calibration curve for Ket

2.5 Characterization techniques

X-ray powder diffraction (XRD) patterns were recorded on a Bruker AXS D8 diffractometer using monochromatic CuK α radiation ($\lambda = 0.154$ nm), operating at 40 kV and 50 mA over a 2θ range from 4 to 70°. FTIR spectra were recorded on a FT-IR Bomem MB 104 spectrometer under the following experimental conditions: 200 scans in the mid-IR range (400–4000 cm^{-1}) using KBr (ratio 5/95 wt%) pellets, and a resolution of 4.0 cm^{-1}.

2.6 In vitro Ket release study

The release of Ket from ZnAlLDH_Ket and MgAlLDH_Ket into the media (phosphate buffer solution pH 7.4) was performed using the continuous method described in our previous paper [25].

The sample amount was 0.1 g and the buffer solution volume was 100 ml. The study was performed at 37°C. The flow rate was 0.5 ml/min and respectively 1.0 ml/min. The release kinetics of Ket has been followed for 18 h. The amount of Ket released into the solution was determined by using UV-visible spectrophotometer analysis at 255 nm wavelength.

After the kinetic studies the recovered solid samples were washed twice, each time using a volume of 100 ml deionized water, then dried and characterized by DRX and FTIR techniques.

2.7 In vivo study of gastrointestinal tolerance and analgesic effect

Two types of in vivo pharmacological studies were performed: the gastrointestinal tolerance and the analgesic effect evaluation of the Ket intercalated into LDHs. The choice of animal model consisted in mice models for determining the gastrointestinal tolerance [14, 20, 21, 26–29] and antinocieptive mice models for evaluating the analgesic effect [26, 30–32]. A total of 68 animals were used in the study.

2.7.1 Animal study

The study was conducted on Swiss mice, adult males, with an average weight of 20 g (± 2 g), provided by the animal breeding facility of the Central Laboratory for Drug Testing, "Grigore T. Popa" University of Medicine and Pharmacy, Iasi.

The animals were maintained in a temperature controlled room (21°C $\pm$ 2°C) with a 12 h/12 h light/dark cycle, 4 mice per cage. The animals were allowed to get used with the environment for at least 24 h before testing, with unlimited access to water. Access to food was stopped

16 h before receiving the drug sample. At the end of the study, the animals were euthanized according with European regulations, without any suffering.

The research activity on the laboratory animals (handling, feeding, killing, chronic treatments, etc.) was conducted according to the bioethics rules endorsed by European Union legislation (Directive of the EU Council no. 609 from 24 November 1986) and by the IASP Committee on Ethical Issues: recommendations from the "Declaration of Helsinki"; "Guiding Principles in the Care and Use of Animals" approved by the American Physiological Society and the Ethical Guidelines for Investigations of Experimental Pain in Conscious Animals [33]. These guidelines and rules were included in standard protocols and approved by the Bioethics Committee of the "Gr. T. Popa" University of Medicine and Pharmacy Iasi.

2.7.2 Pharmacological studies for determining the gastrointestinal tolerance

The samples (pure Ket, LDHs, ZnAlLDH_Ket and MgAlLDH_Ket) were delivered orally (80 mg active ingredient/kg weight of mouse) to different groups of animals. The compounds, each dispersed in 1 ml saline, were administered per os (p.o.). The ZnAlLDH_Ket and MgAlLDH_Ket composite sample amounts were adjusted to deliver the equivalent Ket dose of 80 mg/kg b.w.

2.7.3 Evaluation of gastrointestinal tolerance

The total number of animals involved in the gastrointestinal tolerance study was 32. They were divided into 4 groups, 8 animals per group. Each group received one of the following treatments: saline (control group), pure Ket, ZnAlLDH_Ket or MgAlLDH_Ket respectively, in the dose and volume described above.

The mice were euthanized 24 h after the sample administration. The abdominal cavity was surgically cut open, followed by careful extraction of the stomach and of jejunum and ileum fragments. Tissue portions were thoroughly exposed and fixed on a solid support to reveal the lesions. The surface of mucosa was rinsed with saline solution before evaluation.

To quantify the extension of the mucosal lesions, tissue samples were observed with a magnifying glass equipped with an optical zoom of X10. The lesions were quantified according to the following scoring system: 1 = erosion point, 2 = erosion <1 mm, 3 = erosion of 1–2 mm, 4 = erosion of 2–3 mm, 5 = erosion of 3–4 mm, 6 = erosion >4 mm.

For each studied animal, a score was assigned, calculated by summing up the points given for the diameter of

each lesion separately. An average score was calculated for each group.

2.7.4 Antinociceptive testing

A total number of 36 animals were used in this study. They were divided into 6 groups, containing 6 animals each. Each group received one of the following treatments: saline (control group), pure Ket, ZnAlLDH_Ket, MgAlLDH_Ket, ZnAlLDH or MgAlLDH respectively, in the dose and volume described in Sect. 2.7.2.

The analgesic effect was measured by nociceptive stimulation through thermo-algesic mechanism (Hot Plate test).

For the hot-plate latency test, a rectangular metal surface was heated to a temperature of $55 \pm 0.5°C$. The antinociceptive response was monitored from the time the mouse was placed on the heated surface until the first overt behavioral sign of nociception (paw withdrawal latency) occured, such as (i) the mouse licking a hind paw, (ii) the mouse shaking a hind paw, (iii) an escape response. Upon the occurrence of any of these signs, the timer was stopped by a foot-operated pedal and the mouse was immediately removed from the plate. Maximum latency (cut-off time) was set at 60 s in order to prevent tissue damage to the back paws. Testing was performed prior to sample administration (time 0), and then at intervals of 30, 60, 90, 120, 180 and 210 min after the treatment in the case of the samples administered orally. Samples that produced a significant increase in the latency response in hot plate test were considered to be antinociceptive.

2.7.5 Statistical analysis

The data was analyzed and reported as mean $\pm$ SD/SE for each determination. Differences between treated groups are analyzed using ANOVA one-way method, followed by Bonferroni post-hoc test. Values of the P coefficient less than 0.05 were considered to indicate a statistically significant difference in all tests.

3 Results and discussion

3.1 Elemental analysis and spectrophotometric results

Both analysis methods used for determining the amount of intercalated Ket yielded the same results (Table 1). The percentage of intercalated Ket was 46.1% for ZnAlLDH_Ket and 50.1% for MgAlLDH_Ket respectively (by total sample weight), reported as an average value of the two analysis methods.

Table 1 Ket content in LDH_Ket samples, determined by elemental and spectrophotometric analysis

Sample	Elemental analysis		Spectrophotometric analysis
	C (%)	Ket (%)	Ket (%)
ZnAlLDH_Ket	35.4	46.9	45.2
MgAlLDH_Ket	37.8	50.0	50.2
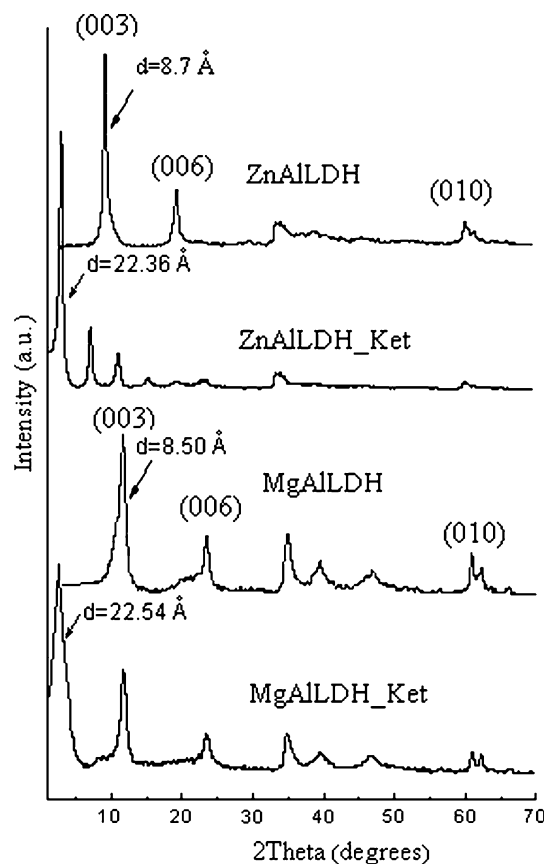
Fig. 2 Comparative powder XRD patterns for: ZnAlLDH, ZnAlLDH_Ket, MgAlLDH and MgAlLDH_Ket

3.2 Powder X-ray diffraction

The powder X-ray diffraction (XRD) patterns of the precursor ZnAlLDH, MgAlLDH and its hybrids ZnAlLDH_Ket and MgAlLDH_Ket are shown in Fig. 2. The diffractograms recorded for LDHs precursors (Fig. 2) show typical layered structures similar to those reported in the literature for this type of materials [34, 35].

The basal spacing of ZnAlLDH and MgAlLDH with nitrate as inter lamella anion is 8.74 and 8.50 Å, respectively. These values correspond to the expected basal spacing of nitrate anion incorporated in hydroxide layer [36]. The magnitude of the basal spacing found in hydrotalcite samples increases upon the inclusion of Ket into the

LDH lamella. This trend is shown in Fig. 2, where the basal spacing of ZnAlLDH_Ket and MgAlLDH_Ket is 22.36 and 22.54 Å, respectively. This expanded interlayer separation is due to the molecular size and geometrical arrangement of Ket in the interlayer space. These results are in good agreement with those reported in the literature regarding intercalation of organic anions of similar size to Ket. For example upon intercalation of diclofenac, 4-biphenylacetic acid, mefenamic acid, meclofenamic acid and ibuprofen anions the expanded interlayer spacing was in the range of 20.4 to 23.2 Å [13, 14, 17, 19, 37].

3.3 FTIR spectroscopy

FT-IR spectra of Ket, LDHs and LDHs_Ket samples are presented in Fig. 3. The results confirm the intercalation of Ket in the MgAlLDH and ZnAlLDH lamella. The recorded FT-IR spectrum of pure Ket (Fig. 3), shows characteristic vibration bands associated with its structure [38].

The main peaks correspond to the following frequencies: 2990–2878 cm^{-1} (methyl v-CH), above 3018 cm^{-1} (aromatic ring v-CH), 1697 cm^{-1} (carbonyl vC=O), 1655 cm^{-1} (vC=O, stretching of the ketone) 1597, 1585 and 1445 cm^{-1} (aromatic ring vC=C) [3].

In the FT-IR spectra of ZnAlLDH and MgAlLDH, the broad and strong band located in the frequency range of 3600–3200 cm^{-1} and centered at 3431 cm^{-1}, is a common feature for all the hydrotalcite-type materials corresponding to the OH stretching vibration due to the presence of water molecules [39]. The bands observed in the low-frequency region of the spectrum are associated as the lattice vibration modes and can be attributed to M–O from 850 to 600 cm^{-1} and M–O–M near 426 cm^{-1} (M = Al, Zn, Mg) in the LDH sheets [40]. The appearance of a strong band at 1381 cm^{-1} is due to the symmetric vibration of the interlayer nitrate anion from MgAlLDH and ZnAlLDH [41].

All the vibration bands associated with the organic anion are found in the spectra of the samples containing intercalated Ket, together with the absorption bands characteristic for LDHs (Fig. 3).

The band characteristic for the C=O group is located at 1655 cm^{-1} and the band assigned to the C=C bond in the Ket aromatic ring is located at 1554 cm^{-1}. The absence of the band at 1381 cm^{-1} in the spectrum of MgAlLDH_Ket and ZnAlLDH_Ket, confirms the fact that the interlayer nitrate anions have been displaced.

3.4 Kinetic study

The in vitro release of Ket from LDHs nanohybrid material was investigated under simulated conditions mimicking the gastrointestinal tract environment [42–46].

The amount of Ket released from the samples was calculated as:

$$m_{Ket} = c_d V_e + \sum_{i=0}^{n-1} c_i V_i \tag{2}$$

where m_{Ket} is the amount of Ket released from the sample at a certain time (mg); c_d is the concentration of drug in the extracted sample (μg/ml); V_e is the volume of eluent from the system; V_i is the volume of extracted sample, i; and c_i is the concentration of Ket in the extracted sample, i, (μg/ml) determined spectophotometrically.

Figure 4 shows the release profile of Ket from ZnAlLDH_Ket and MgAlLDH_Ket into the buffer solution pH 7.4 and different flow-rates. Each point represents the calculated average of three measurements. The accumulated Ket released into the aqueous solution increased with contact time and flow-rate when LDHs_Ket were placed in contact with aqueous solution.

When the matrix is relatively stable in the elution medium, it is expected that the drug diffusion is the rate determining step for the release kinetics. Therefore the empirical equation developed by Ritger and Peppas [47] can be applied in order to obtain the diffusion parameters from the early stage release data:

$$\frac{M_t}{M_\infty} = kt^n \tag{3}$$

where M_t/M_∞ represents the fraction of released drug at time t, k is a constant characteristic to the drug-LDH interaction and n is an empirical parameter characteristic to the release mechanism. When ln (M_t/M_∞) is plotted versus
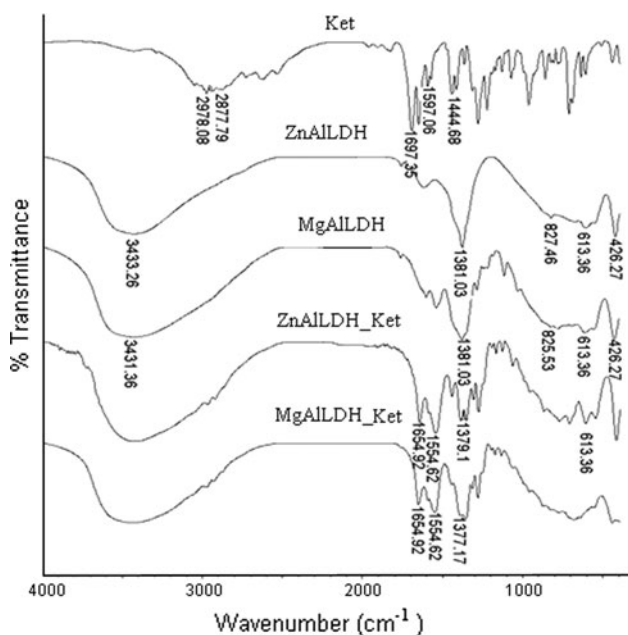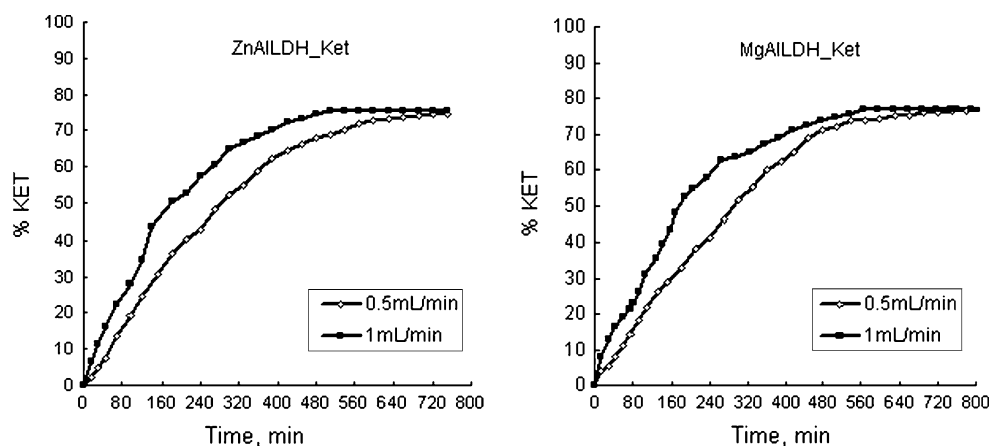

Fig. 3 Comparative FTIR spectra for: Ket, ZnAlLDH, MgAlLDH, ZnAlLDH_Ket and MgAlLDH_Ket

**Fig. 4** Release profiles of Ket from: ZnAlLDH_Ket and MgAlLDH_Ket into the aqueous solutions at initial pH 7.4

$\ln(t)$, the value of the diffusional exponent is obtained. According to Lee and Jou [48], the diffusion relative rate and relaxation process cause three different classes of diffusion, characterized by distinct values of the diffusional exponent. When $n = 0.5$ the rate of diffusion is much smaller than the rate of relaxation and the process is called Fikian diffusion. Secondly, if $n = 1.0$, the diffusion process is much faster than the relaxation phenomena. In this case the controlling step is the velocity of the advancing front, which forms the boundary between the swollen outside layer and the glassy core. Thirdly, in non-Fickian diffusion ($n = 0.5$–1.0) the diffusion and relaxation rates are comparable.

In this work the n parameters were calculated from the plot of $\ln(M_t/M_\infty)$ versus $\ln(t)$ (Fig. 5) using the obtained experimental data.

The calculated value of n parameter is approximately equal to 1 for the two types of layered double hydroxides when the flow-rate is 0.5 ml/min. Under these conditions the release rate is controlled by the ion exchange process between the Ket anion intercalated into LDH and phosphate ions from release environment. At a flow-rate of 1.0 ml/min, the calculations yield $n = 0.80$ for ZnAlLDH_Ket complex and $n = 0.72$ for MgAlLDH_Ket complex respectively. In this case the diffusion rate is comparable with the ion exchange reaction rate of the anions involved in the process.

In order to obtain some information about the release mechanism, we subsequently recovered the residue left in the aqueous solution after the Ket release experiment. The DRX patterns for MgAlLDH_Ket and ZnAlLDH_Ket (residue recovered after release process) are presented in Fig. 6.

The distance between layers of the residue analyzed after release was 11.63 Å for MgAlLDH_Ket and 10.37 Å for ZnAlLDH_Ket. These values are in agreement with expectation for the layered double hydroxides containing phosphate ions intercalated between layers [49].
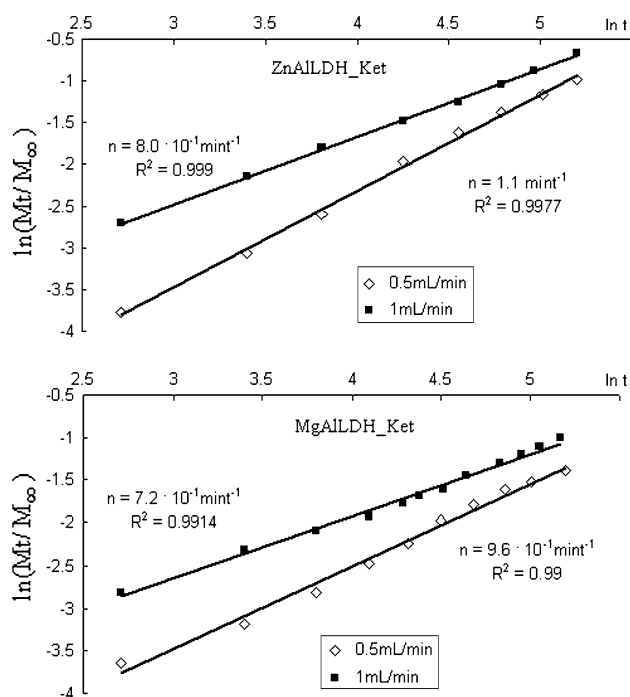

Fig. 5 Comparative plots of $\ln(M_t/M_\infty)$ versus $\ln(t)$ for: ZnAlLDH_Ket and MgAlLDH_Ket

In the FTIR spectra recorded after drug release (residue recovered after release process) at pH 7.4 (Fig. 7), the characteristic bands of Ket disappear, the specific bands of layered double hydroxides are restored and a new band appears at 1050 cm^{-1} that is characteristic to the presence of phosphate ion. Both DRX and FTIR analysis methods suggest that drug release from hybrids with Ket, is due to the ion exchange process between Ket anions and phosphate ions belonging to the elution medium.

3.5 Evaluation of gastrointestinal tolerance

The administration of a single dose of 80 mg/kg p.o Ket in mice causes significant gastric irritation effects. The gastric
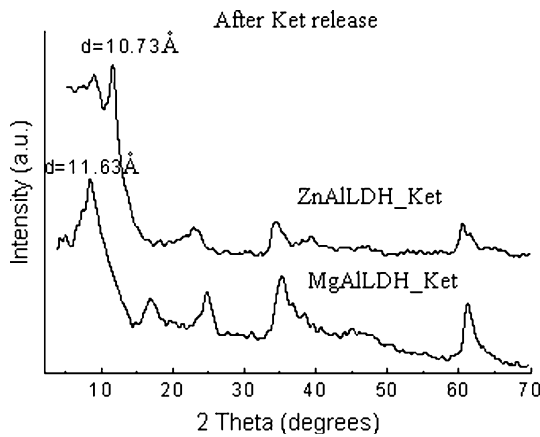
Fig. 6 Comparative DRX patterns obtained for solid residue left after the release of Ket from: MgAlLDH_Ket and ZnAlLDH_Ket
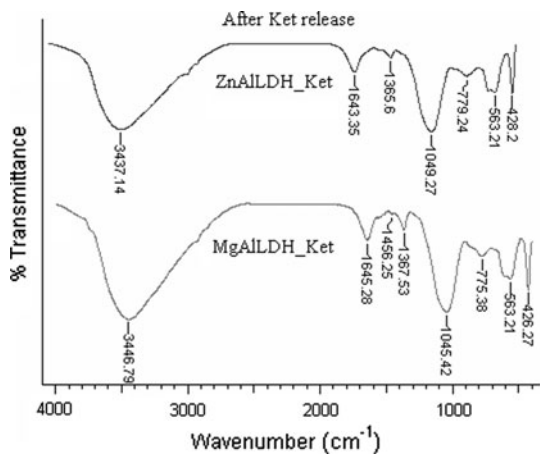

Fig. 7 Comparative FTIR spectra obtained for solid residue left after the release of Ket from: MgAlLDH_Ket and ZnAlLDH_Ket

mucosa has an edematous aspect, with areas of micro-hemorrhages and erosion points. The lesions are present both in the stomach, jejunum and in the ileum.

Administration of Ket intercalated with the chosen versions of hybrid materials, LDHs_Ket, causes an irritation syndrome significantly lower when compared with the group that received matrix free Ket. Although the incorporation in the matrix significantly reduced the lesions in number and size when compared to the group that received raw Ket, certain micro erosions were still found in all three types of gastrointestinal tissue segments (stomach, jejunum and ileum) following the administration of ZnAlLDH_Ket. Errosions are missing or barely visible in stomachs of mice that received MgAlLDH_Ket (Fig. 8). These results are in accordance with the phenomena observed in the preliminary studies with these materials [26].

Compared to the ZnAlLDH, the inclusion of Ket in MgAlLDH provides better protection, with normal
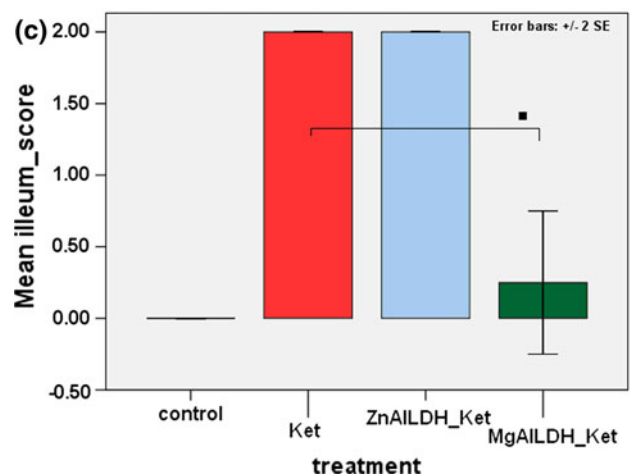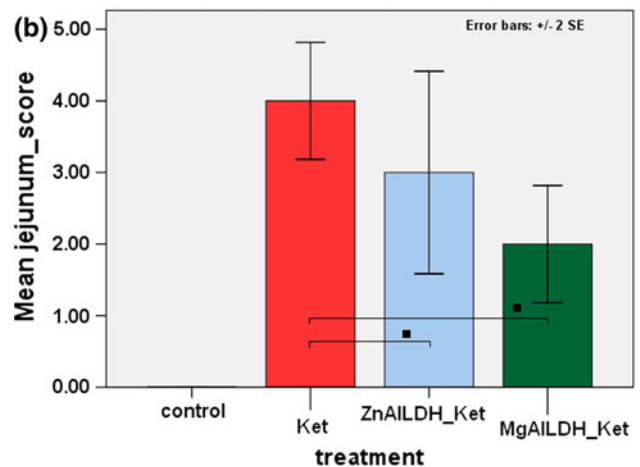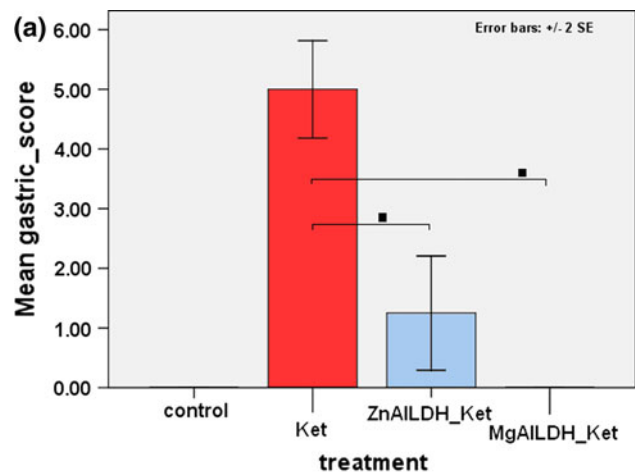
Fig. 8 Evaluation of gastrointestinal tolerance. The quantified score: gastric score (a), jejunum score (b), ileum score(c) ($n = 8$ for each treatment group)

appearance of the digestive mucosa, even when the high Ket doses were used.

Therefore, the results obtained on the two newly synthesized versions of LDHs showed good local gastric tolerance, revealed by the normal aspect of the macroscopically

analyzed gastric mucosa (Fig. 9). Erosion or hemorrhagic points are marked by arrows and very pronounced on Ket images, barely visible on ZnAlLDH_Ket and missing on MgAlLDH_Ket, reinforcing the information provided by the scores reported in Fig. 8.

The significant difference observed between the raw Ket and the LDH incorporated Ket is due to the fact that the
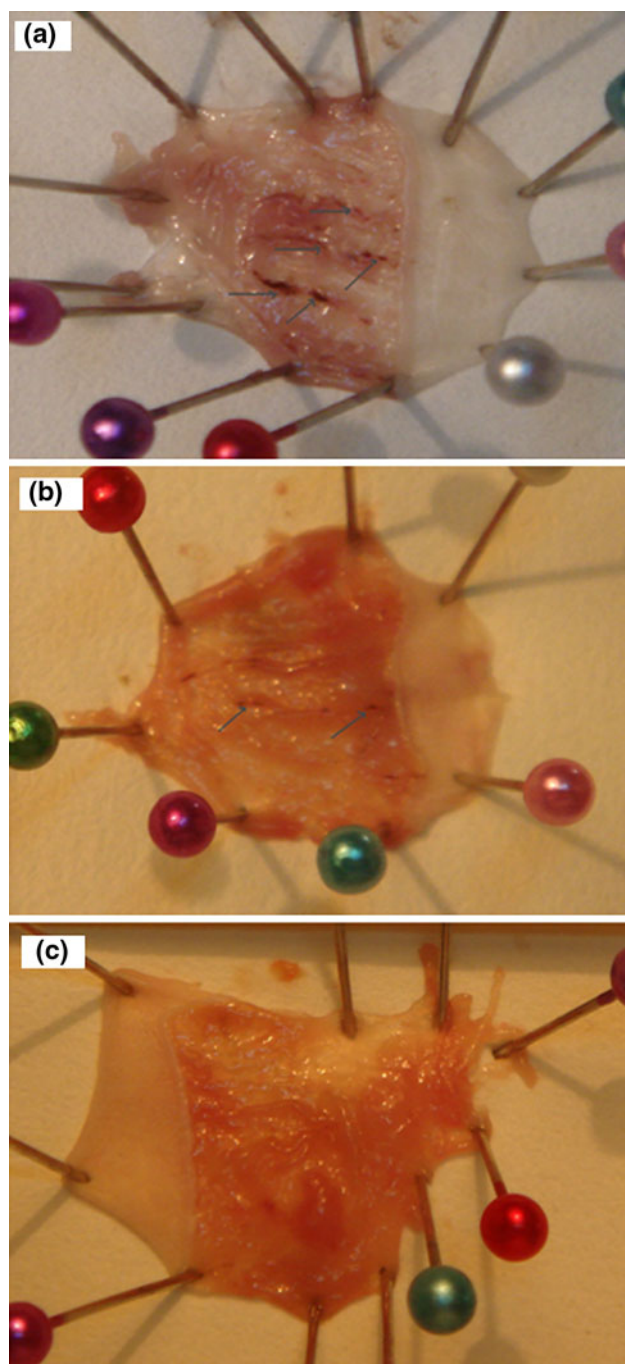
Fig. 9 Photographs of extracted stomachs after treatment with: Ket (a), ZnAlLDH_Ket (b), MgAlLDH_Ket (c); *arrows* indicate erosion/hemorrhagic points

hydrotalcites not only have the capability to neutralize acids, but also are known to inhibit pepsin action at pH values at which its activity is still high [50–52]. Recent studies have also shown that hydrotalcites are responsible for an activation mechanism that takes place in the gastric mucosa and is related to genes encoding for the epidermal growth factor and its receptor. This observation might provide a physiological basis for an ulcer healing action [53].

3.6 Antinociceptive testing

The oral administration of raw LDH did not significantly influence the response latency to thermal nociceptive stimuli. Orally administered doses of 80 mg/kg Ket significantly increased the response latency (Fig. 10).

The observed antinociceptive effect of both versions of intercalated Ket into LDHs is significant when compared to both the records obtained before the administration of samples and records measured in the control group.

Both combinations of Ket with LDH induced an analgesic effect comparable in intensity and duration with the matrix-free Ket group. The antinocieptive effect of the MgAlLDH_Ket retains a significant value of analgesia for a longer period of time compared to the ZnAlLDH_Ket compound.

The MgAlLDH_Ket formulation shows a tendency towards a stronger antinociceptive effect than the ZnAlLDH_Ket counterpart during the 210 min recorded period.

4 Conclusions

Ket intercalation in LDH's was achieved by ion exchange and confirmed by DRX and FTIR analyses. The in vitro study at pH 7.4 showed that the Ket release kinetics and mechanism depend on the eluent flow rate. On one hand, the release rate is controlled by the ion exchange process between the intercalated Ket anions and the phosphate ions belonging to the eluent when the flow rate equals 0.5 ml/min. On the other hand, the Ket diffusion rate becomes comparable to the ion exchange process when the flow rate reaches 1 ml/min.

The most significant downside of chronic clinical use of NSAIDs is the irritation syndrome at the level of gastro-intestinal mucosa, where erosions and hemorrhagic lesions have been frequently described. The in vivo gastric tolerance study was aimed at evaluating LDH's capacity of protecting against this side effect of NSAIDs.

In our study, during the in vivo gastric tolerance tests, the intercalated ketoprofen created fewer and smaller lesions than its raw counterpart. This result is in agreement

Fig. 10 Quantification of analgesic activity by thermo-algesic nociception test (hot plate) at i.p injection of Ket, ZnAlLDH_Ket, MgAlLDH_Ket, ZnAlLDH, MgAlLDH ($n = 6$ for each treatment group)
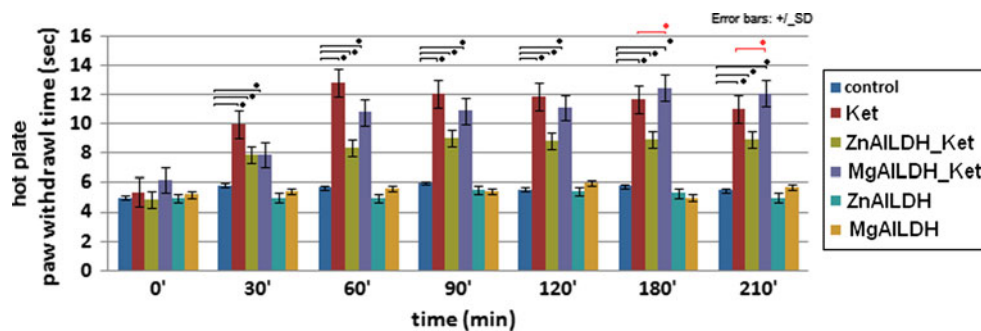
with the other in vivo studies describing hydrotalcite and other aluminium based antacids as exercising a significant protecting activity of gastrointestinal mucosa, against lesions induced by nonsteroidal anti-inflammatory drugs and ethanol [20, 21, 26, 29]. Similar data were previously reported for another propionic acid derivative, the NSAID indomethacin, when intercalated into LDH's [14].

Our in vivo studies over the analgesic efficacy of the new Ket intercalated into LDHs formulations demonstrated a slightly higher antinocieptive effect, maintained for longer periods of time when compared with Ket alone.

Among the two proposed formulations, MgAlLDH_Ket showed a stronger antinociceptive effect that was sustained for a longer period of time than the ZnAlLDH_Ket.

Future studies will be aimed at determining the kinetic profile of in vivo Ket release from LDHs_Ket composites.

References

1. Heyneman CA, Lawless-Liday C, Wall GC. Oral versus topical NSAIDs in rheumatic disease: a comparison. Drugs. 2006;60:555–74.
2. Marie RG. Epidemiology of nonsteroidal anti-inflammatory drug-associated gastrointestinal injury. Am J Med. 1998;104:23S.
3. Vueba ML, Pina ME, Veiga F, Sousa JJ, Batista de Carvalho LAE. Conformational study of ketoprofen by combined DFT calculations and Raman spectroscopy. Int J Pharm. 2006;307:56–65.
4. Kantor TG. Ketoprofen: a review of its pharmacologic and clinical properties. Pharmacotherapy. 1986;6:93–103.
5. Marie RG. Nonsteroidal anti-inflammatory drugs: practical and theoretical considerations in their selection. Am J Med. 1996;100:31S.
6. Savage RL, Moller PW, Ballantyne CL, Wells JE. Variation in the risk of peptic ulcer complications with nonsteroidal antiinflammatory drug therapy. Arthritis Rheum. 1993;36:84–90.
7. Babazadeh M. Synthesis and study of controlled release of ibuprofen from the new acrylic type polymers. Int J Pharm. 2006;316:68–73.
8. Bonina FP, Puglia C, Barbuzzi T, Caprariis PD, Palagiano F, Rimoli MG, Saija A. In vitro and in vivo evaluation of polyoxyethylene esters as dermal prodrugs of Ketoprofen, naproxen and diclofenac. Eur J Pharm Sci. 2001;14:123–34.
9. Costantino U, Ambrogi V, Nocchetti M, Perioli L. Hydrotalcite-like compounds: versatile layered hosts of molecular anions with biological activity. Microporous Mesoporous Mater. 2008;107:16–149.
10. Frunza M, Hritcu D, Popa MI. Intercalation of salicylic acid into ZnAl layered double hydroxides by ion-exchange and coprecipitation method. J Optoelectron Adv Mater. 2009;11:528–34.
11. Ko JA, Park HJ, Hwang SJ, Park JB, Lee JS. Preparation and characterization of chitosan microparticles intended for controlled drug delivery. Int J Pharm. 2002;249:65–74.
12. Liu Z, Jiao Y, Wang Y, Zhou C, Zhang Z. Polysaccharides-based nanoparticles as drug delivery systems. Adv Drug Deliv Rev. 2008;60:1650–62.
13. del Arco M, Gutiérrez S, Martín C, Rives V, Rocha J. Synthesis and characterisation of layered double hydroxides (LDH) intercalated with non-steroidal anti-inflammatory (NSAID) drugs. J. Solid State Chem. 2004;177:3954–62.
14. del Arco M, Cebadera E, Gutirrez S, Martin C, Montero MJ, Rives V, Rocha J, Sevilla MA. Mg, Al layered double hydroxides with intercalated indomethacin: synthesis, characterisation and pharmacological study. J Pharm Sci. 2004;93:1649–58.
15. del Arco M, Fernandez A, Martin C, Rives V. Release studies of different NSAIDs encapsulated in Mg, Al, Fe-hydrotalcites. Appl Clay Sci. 2009;42:538–44.
16. Frunza M, Popa MI, Hulea V. Controlled release of salicylate from the lamella Zn-Al layered double hydroxide nanocomposite. J Optoelectron Adv Mater. 2007;9:3376–8.
17. Frunza M, Lisa G, Zonda R, Popa MI. Intercalation of Ketoprofen into Mg-Al hydrotalcites. Synthesis and characterization. Rev Chim-Bucharest. 2008;59:409–12.
18. Li B, He J, Evans DG, Duan X. Inorganic layered double hydroxides as a drug delivery systems intercalation and in vitro release of fenbufen. Appl Clay Sci. 2004;27:199–207.
19. Silion M, Popa MI, Lisa G, Hritcu D. New hybrid compounds containing intercalated ciprofloxacin into layered double hydroxides: synthesis and characterization. Rev Roum Chim. 2008;53:827–31.
20. del Hoyo C. Layered double hydroxides and human health: an overview. Appl Clay Sci. 2007;36:103–21.
21. Tarnawski AS, Ahluwalia A, Gandhi V, Deng X, Xiong X. Hydrotalcite protects aging gastric mucosa against NSAID- and ethanol-induced injury by preserving endothelial and progenitor cells. Underlying molecular mechanisms include activation of survivin and VEGF. Gastroenterology. 2010;138:S-721.
22. Yu BP, Sun J, Li MQ, Luo HS, Yu JP. Preventive effect of hydrotalcite on gastric mucosal injury in rats induced by taurocholate. World J Gastroenterol. 2003;9:1427–30.
23. Carlino S. The intercalation of carboxylic acids into layered double hydroxides: a critical evaluation and review of the different methods. Solid State Ionics. 1997;98:73–84.

24. Silion M, Popa MI. Preparation and characterization of keto-profen-layered double hydroxide compounds. J Optoelectron Adv Mater. in press 2010.

25. Beldie C, Dumitriu S, Aelenei N, Popa M, Popa MI, Bioactive DumitriuD, Polymers LX. Kinetics of delayed release neomycin-xanthan complex. Biomaterials. 1989;10:622–4.

26. Jaba IM, Ionescu D, Popa MI, Silion M, Tamba B, Mungiu OC. The analgesic effect and local tolerance of new anorganic nanohybrid systems with ketoprofen. InfoMedica. 2008;3:10–3.

27. Tuo B, Wen G, Wang X, Liu X, Dong H. Estrogen potentiates prostaglandin E2-stimulated duodenal mucosal bicarbonate secretion in mice. Gastroenterology. 2010;138:S-721.

28. Krylova SG, Fomina TI, Efimova LA, Zueva EP, Khotimchenko MIu, Razina TG, Amosova EN, Lopatina KA, Khotimchenko IuS. Antiulcer effect of calcium pectate on model of chronic gastric ulcer in rats. Eksp Klin Farmakol. 2009;72:35–8.

29. Konturek SJ, Brzozowski T, Garlicki J, Majka J, Stachura J, Nauert C. Intragastric pH in the gastroprotective and ulcer-healing activity of aluminum-containing antacids. Digestion. 1991; 49:140–50.

30. Carstens E. Quantitative experimental assessment of pain and hyperalgesia in animals and underlying neural mechanisms. In: Carli G, Zimmermann M, editors. Progress in Brain Research, vol 110. Amsterdam: Elsevier Science B.V. 1996. p. 17–31.

31. Derbyshire SWG. Assessing pain in animals. In: Basbaum AI, Kaneko A, Shepherd GM, Westheimer G, Albright TD, Masland RH, Dallos P, Oertel D, Firestein S, Beauchamp GK, Bushnell MC, Kaas JH, Gardner Esther, editors. The senses: a comprehensive reference, vol. 5. Oxford: Elsevier Inc; 2008. p. 969–74.

32. Williams M. Use of animal models for drug discovery. In: Enna SJ, Bylund DB, editors. xPharm: the comprehensive pharmacology reference. New York: Elsevier; 2008. p. 1–7.

33. Hunskaar S, Hole K. The formalin test in mice: dissociation between inflammatory and non-inflammatory pain. Pain. 1987;30:103–14.

34. Olanrewaju J, Newalkar BL, Mancino C, Komrneni S. Simplified synthesis of nitrate form of layered double hydroxide. Mater Lett. 2000;45:307–10.

35. Xu ZP, Zeng HC. Sulfate-functionized carbon/metal-oxide nanocomposites from hydrotalcite-like compounds. Nano Lett. 2001;1:703–6.

36. Xu ZP, Zeng HC. Abrupt structural transformation in hydrotalcite-like compounds $Mg_{1-x}Al_x(OH)_2(NO_3)_x \cdot nH_2O$ as a continuous function of nitrate anions. J Phys Chem B. 2001;105:1743–9.

37. del Arco M, Fernández A, Martín C, Rives V. Intercalation of mefenamic and meclofenamic acid anions in hydrotalcite-like matrices. Appl Clay Sci. 2007;36:133–40.

38. Maestrelli F, Zerrouk N, Cirri M, Mennini N, Mura P. Microspheres for colonic delivery of ketoprofen-hydroxypropyl-β-cyclodextrin complex. Eur J Pharm Sci. 2008;34:1–11.

39. Cavani F, Trifiro F, Vaccari A. Hydrotalcite-type anionic clays: preparation, properties and application. Catal Today. 1991;11: 173–301.

40. Kanan S, Swamy CS. Synthesis and physicochemical characterization of cobalt aluminium hydrotalcite. J Mater Sci Lett. 1992;11:1585–7.

41. Xu ZP, Zeng HC. Interconversion of brucite-like and hydrotalcite-like phases in cobalt hydroxide compounds. Chem Mater. 1999;11:67–74.

42. Aelenei N, Popa MI, Novac O, Lisa G, Balaita L. Tannic acid incorporation in chitosan-based microparticles and in vitro controlled release. J Mater Sci Mater Med. 2009;20:1095–102.

43. Dashevsky A, Mohamad A. Development of pulsatile multiparticulate drug delivery system coated with aqueous dispersion Aquacoat® ECD. Int J Pharm. 2006;318:124–31.

44. Mastiholimath VS, Dandagi PM, Jain SS, Gadad AP, Kulkarni AR. Time and pH dependent colon specific, pulsatile delivery of theophylline for nocturnal asthma. Int J Pharm. 2007;28:49–56.

45. Rokhade AP, Shelke NB, Patil SA, Aminabhavi TM. Novel interpenetrating polymer microspheres of chitosan and methylcellulose for controlled release of theophylline. Carbohydr Polym. 2007;69:678–87.

46. Serra L, Domenech J, Peppas NA. Drug transport mechanisms and release kinetics from moleculary designed poly(acrylic acid-g-ethylene glycol) hydrogels. Biomaterials. 2006;27:5440–51.

47. Ritger PL, Peppas NA. A simple equation for description of solide release. II. Fickian and anoumalous release from swellable devices. J Control Release. 1987;5:37–42.

48. Lee WF, Jou LL. Effect of the intercalation agent content of montmorillonite on the swelling behavior and drug release behavior of nanocomposite hydrogels. J Appl Polym Sci. 2004; 94:74–82.

49. Costantino U, Casciola M, Massinelli L, Nocchetti M, Vivani R. Intercalation and grafting of hydrogen phosphates and phosphonates into synthetic hydrotalcites and a.c.-conductivity of the compounds thereby obtained. Solid States Ionics. 1997;97: 203–12.

50. Playle AC, Gumming SR, Llewellyn AF. The in vitro antacid and anti pepsin activity of hydrotalcite. Pharm Acta Helv. 1974;49: 298–302.

51. Pawlaczyk J, Kokot Z, Rafinska A. In vitro study of the antipeptic activity of antacid preparations. Acta Pol Pharm. 1985;42:153–8.

52. Dreyer M, Marwinski D, Wolf N, Damman HG. Acid suppression profile of hydrotalcite in man. Arzneim-Forsch. 1991;41:738–41.

53. Tarnawski AS, Tomikawa M, Ohta M, Sarfeh IJ. Antacid talcid activates in gastric mucosa genes encoding for EGF and its receptor. The molecular basis for its ulcer healing action. J Physiol Paris. 2000;94:93–8.